A GPR SURVEY FOR WATER EXPLORATION IN A CRYSTALLINE ROCK TERRAIN

Jandyr Menezes Travassos(1) & Paulo de Tarso Luiz Menezes(2)

Abstract - The vast majority of mineral water occurrences in Brazil are associated to fractures zones in crystalline rocks. Underground water exploration is usually based on geological studies (photo-interpretation) combined with geophysical surveys, mainly electrical methods and VLF.

In this paper we demonstrate the use of GPR method in the exploration of underground water in crystalline terrain. An example of data collected at one known spring in the district of Petrópolis is given. Petrópolis is a major producer in the Rio de Janeiro State. The saturated region is clearly outlined in the GPR section as a zone of attenuation and inversion of the wavelet phase polarity.

Key-words - GPR, underground water

INTRODUCTION

The market for mineral water is increasing at a rate of 3% a year with perspective of increase in the demand (DNPM 1997). The production of mineral water is important for the economy of several districts in the Country. According to DNPM there are 307 sources of mineral water being exploited in Brazil (DNPM 1997). The main producing regions are located in States of São Paulo, Minas Gerais, Pernambuco and Rio de Janeiro (Martins et.al. 1997).

The available data indicates that virtually the totality of the Brazilian occurrences of mineral water are located in faults and fractures in crystalline rock (DNPM 1997). It is important to mention here that about 60% of the Brazilian territory, or about 4,600,000

1 CNPq-Observatório Nacional, 20921-400 Rio de Janeiro, Brazil. ☎ 55 21 5807081, FAX 55 21 5853782, email: jandyr@on.br.

2 DGAP/FGEL/UERJ, 20559-900 Rio de Janeiro, Brazil. ☎/FAX 55 21 5877598, email: ptarso@uerj.br.

km^2, is made of crystalline rocks. This indicates the great potential for mineral water exploration on this type of terrain.

The exploration of underground water in crystalline rocks is usually done through the integration of geological methods with extensive use of aerial photos and, more recently, with the use of geophysical methods. The following geophysical methods have been used: electromagnetic methods (La Terra et. al. 1998, Metello et al. 1998), electrical methods (Mello and Mothé Filho 1993, Oliveira 1993, Drews 1998), and magnetic methods (Rigoti et. al. 1998). The GPR method has not been used in the exploration of mineral water in crystalline rocks. However the method GPR has been used extensively in hydrogeologic studies (van Overmeeren, 1994; Beres & Haeni, 1991). In particular it has demonstrated its effectiveness in delimitating aquifers in sedimentary rocks (Cardimona et. al. 1998). In the present work we demonstrate that the GPR method can be highly effective in the exploration of mineral water in crystalline rocks.

GEOLOGICAL SETTING

The studied area is located within the district of Petrópolis in the State of Rio de Janeiro (Fig. 1). The topography is uneven being on the scarp of Serra do Mar chain of mountains, reaching an altitude of 2000 m. The district of Petrópolis is responsible for about 27% of the production of mineral water of the State of Rio de Janeiro (Martins et.al. 1997).

The principal tectonic unit of the region is the Serra dos Órgãos batholith, see Fig. 1. That batholith is made up of granite and gneiss with a granitic and granodioritic composition. The surrounding rocks belong to the Rio Negro Complex, an assemblage of migmatites, gnaisses, gneiss-schist with interleaved quartzite layers (paragneiss). The main rock types in the area are the migmatites and high grade metamorphosed (Amphibolite facies) gneiss-schist, both classified as the Santo Aleixo Unit (DNPM, 1998). The migmatites frequently exhibits estromatic, flebitic and schollen structures and are mainly composed by biotite-hornblende gneiss/amphibolite with interleaved pegmatite layers. The gneiss frequently exhibit structures and foliations in anti-form and syn-form with two independent folding phases. Due to the high metamorphism and intense folding it is very difficult to observe S_0 (original sedimentary bedding). The occurrence of mineral water in the area is usually associated to zones of fractures in the banded and folded migmatite and paragneiss of the Santo Aleixo Unit.

MINERAL WATER CHARACTERISTICS

The main production zone (a total of four springs) is located at 1000 m of altitude, by the scarp of Serra do Mar mountain chain. The physical and chemical characteristics of the mineral water in the region can be found in the literature (Martins et. al. 1997). The water is classified as radioactive at the spring probably due to the radionuclides present in the percolated rocks. The water has a pH of 6.1 at 25°C, and a conductivity of 3.5×10^{-3} mhos/m. The water has 34.8 mg/l of dissolved salts in its composition.

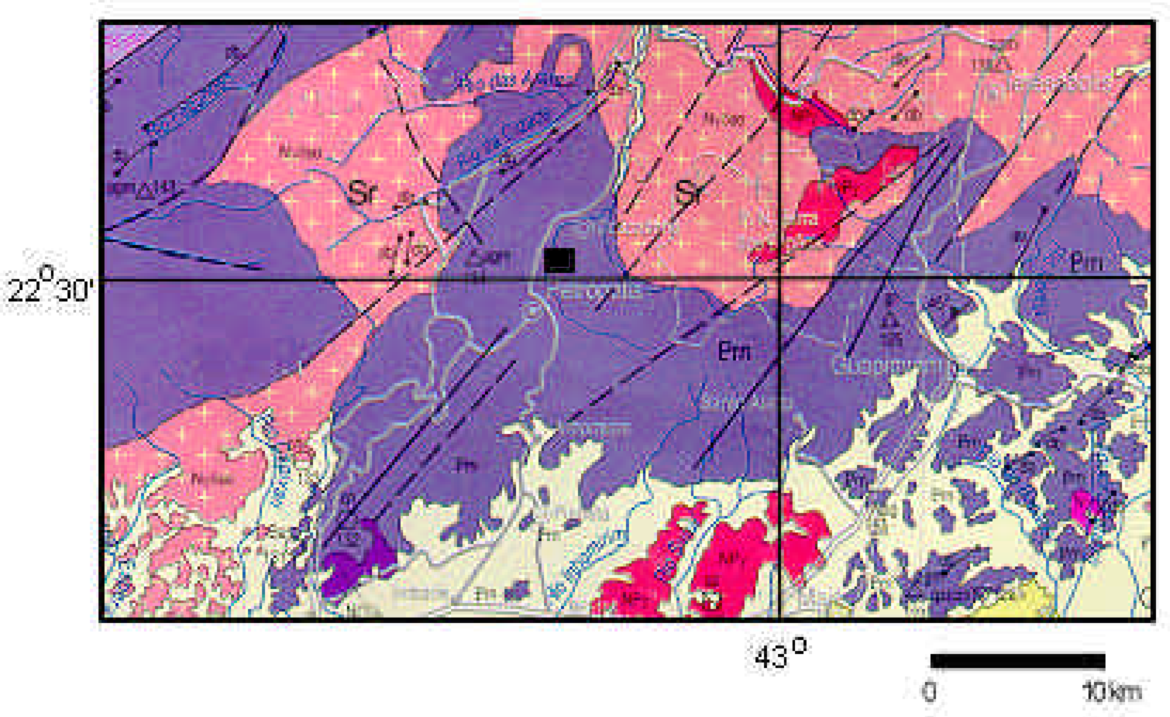

Figure 1. Location of the study area (black square in the center portion of the map) superimposed on a geologic map of the region (DNPM, 1998). Sr – Serra dos Órgãos Batholith. Prn – Rio Negro Complex.

DATA ACQUISITION

Virtually all the data was collected keeping the transmitter and the receiver in the fixed offset configuration. Figure 2 shows a sketch of a fixed offset trace when two targets are imbedded in a uniform background. A GPR section is made up of many traces collected along a profile thus allowing the observer to locate targets. Each new trace is obtained dragging the two antennas together along the profile. The reflected wavelets reflected from two targets appear on the corresponding traces along with increasing time, two-way time or TWT. This is the time it took the pulse to be emitted, to bounce back, and to be recorded at the receiver, as shown in Figure 2. Time (TWT) can be converted to depth if velocity of radar waves in the subsurface is known. An estimate of velocity can be achieved through velocity analysis of CMP (common mid point) sections. In the CMP field configuration the transmitter and receiver are moved away one from the other up to a maximum distance. This distance is a compromise between the investigating depth and the absorption of the electromagnetic waves in the medium.

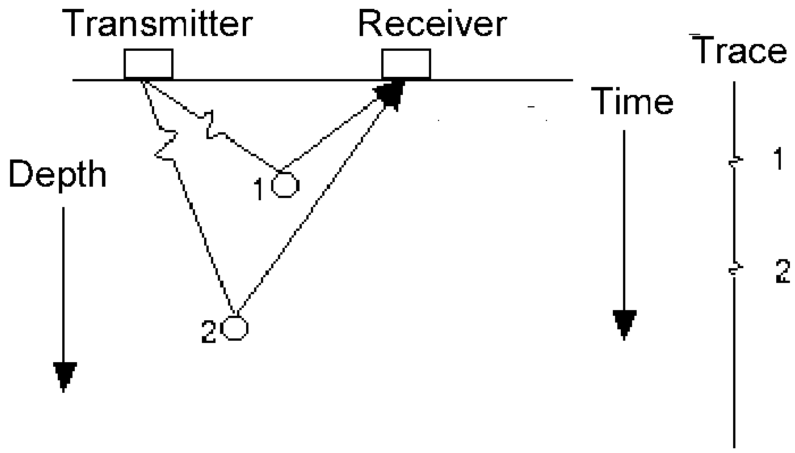

Figure 2. Basic principle of the GPR method. The transmitter antenna emits a pulse that reflects on the two targets (1 and 2) before being recorded by the receiving antenna. The time information in the trace (reflections 1 and 2) can be converted to depth as long as the velocity of electromagnetic waves is known. The antennae can be moved along a profile in fixed offset or in CMP field configurations.

The data was collected with a Pulse Ekko IV GPR (Davis and Annan, 1989) with a 1000 V pulser. The transmitter antenna radiates a broadband wavelet that has an amplitude spectrum as wide as its center frequency: 100 MHz. The transmitting antenna has a broad radiation pattern reaching apertures between 90° and 180°. The bi-static antenna configuration allows a great flexibility of data collection strategies. Antennas were dragged along the profiles with a constant step of 0.20 and 0.25 m. Antennas were dragged keeping their mutual distance constant (fixed offset) or increasing that distance continuously (CMP).

The total time window used in the fixed-offset profiles was 250 ns, enough to reach depths of 10-12 m. That time window however was increased to 350 ns for the CMP profiles.

The whole survey amounted to more than 500 m of fixed-offset reflection profiles mostly deployed on uneven terrain. The spatial density of traces was 0.25 m/trace throughout. The antennae were kept 1 m apart. A section of a 120 m long profile on a relatively flat terrain is used here to illustrate the effectiveness of the GPR to locate water in fractures.

Two 25 m CMP profiles were done in two locations in the survey area in order to estimate an average velocity to be used in the fixed-offset sections. Antennae separation was increased stepwise in increments of 0.1 m from an initial separation of 1 m. The two CMP profiles yielded similar results.

RESULTS

The propagation velocity of radar waves, v_r, is a function of the dielectric constant of the soil. The dielectric constant in turn is affected by water content. The propagation velocity can be determined by CMP measurements. From a CMP section is possible to infer the velocity of the direct waves (in air as well as the groundwave), the velocity of the reflected waves, and of the refracted waves in some special circumstances. Here we concentrate on the velocity of reflected waves.

The reflections from the interfaces between layers with different dielectric constants appear as hyperbolas in CMP sections. This is based on the assumption that the arrival time for signals from reflectors varies hyperbolically with the separation between the transmitter and the receiver. Such assumption remains valid as long as reflectors have small dip. The curvature of a given hyperbola depends on the velocity of the radar waves. Therefore the velocity analysis of a given hyperbola will give an average velocity to the depth of the reflector.

The velocity analysis used here uses the concept of velocity stack in a constant velocity earth. CMP traces are compensated for normal moveout assuming a constant velocity hyperbolic equation. Traces are then stacked. A range of velocity from 0.05 to 0.15 m/ns was covered with increments of 0.01 m/ns. When a given velocity in that range matches the normal moveout velocity, a reflector will stack coherently. This will result in larger amplitude in the stack. On the other hand when a given velocity does not match that of the reflector, traces add together incoherently. This will result in smaller amplitudes.

The velocity analysis of the CMP profiles has given an average velocity of v_r=0.08 m/ns. Figure 2 shows the result of the velocity analysis done on one CMP profile. This velocity is 38 % less than it is usually tabulated for granite-gneiss (0.13 m/ns). This can be attributed to a higher water content in soil and rock. There are two continuous reflectors at 145 and 300 ns, i.e., well below 5 m deep, both yielding the same velocity as it can be seen in Fig. 2.

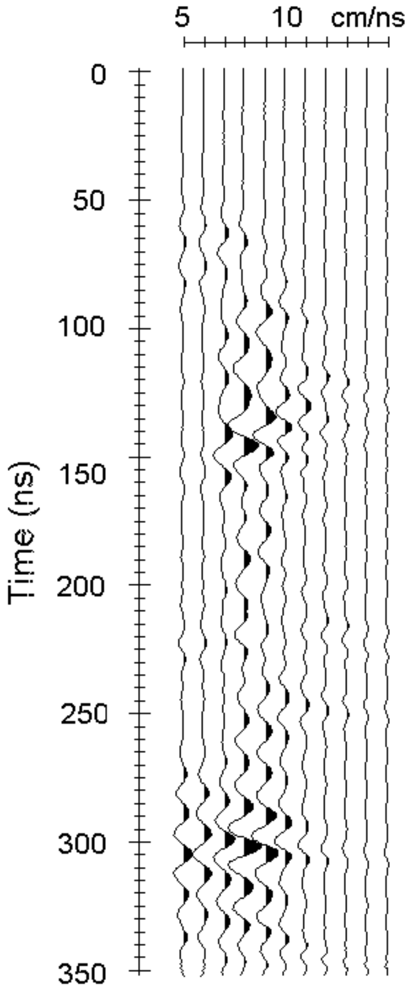

Figure 3. Velocity analysis for the CMP profile. Velocity is incremented in 1 cm/ns steps from 5 to 15 cm/ns.

The velocity in the saprolite layer can be estimated directly from the groundwave signature (a straight line) in the CMP section. The groundwave velocity is about 0.1 m/ns. The maximum thickness of the underground which contributes to the transfer of the direct wave energy is determined by half of the Fresnel zone. The groundwave is better seen until a distance transmitter-receiver of 10 m. Considering this distance, the thickness for 100 MHz is 1.6 m. This is about the thickness of the saprolite in the study area as seen in road cuts. This shows that the velocity model for the study area can be approximated by a two-layer model: a first layer of less than 2 m thick with 0.1 m/ns over a slower half-space of 0.08 m/ns.

The water in the area appears in fractures indicating that our target is not a long and continuous reflector as it would be the case of a water table. Due to the fractures we expect that reflection sections will be cluttered with diffractions. Diffractions are hyperbolic events caused by the discontinuities in the rock that may interfere with each other obscuring the sections. They are a direct consequence of the radiation width, as depicted in Figure 2. Diffractions and interference patterns can be dealt with migration, an imaging technique that focuses the energy along hyperbolas to the true spatial position from which the energy originated. The GPR section in this paper is migrated assuming that the rocks below the saprolitic layer is more or less homogeneous.

In this work we use the f-k migration approach of Stolt (Yilmaz, 1987). It is both assumed that the GPR data can be considered as zero offset and that the average velocity estimated through the velocity analysis above can be taken as a constant background velocity along the profile: v_r=0.08 m/ns. We also have chosen a relatively flat profile to apply the migration. The data is dewowed, clipped, resampled, and tapered before migration.

Figure 4 shows a 70 m section clipped from the 120 m long profile crossing a known spring (32 m). A spreading and exponential compensation gain assuming an attenuation of 0.1 dB/m was applied to the section. Data was low-pass filtered with a cutoff at 250 MHz to reduce high-frequency noise and clipped in time to chop off values at and earlier than the first break. Section was migrated assuming a constant velocity throughout. Water-filled fractured rock can be seen beyond 25 m and below 5 m deep. Water-filled fractured rock appears in the section as a region of lower amplitude reflections. That region gets deeper towards the end of the section, extending to 60 m. Fracture induced diffraction were virtually eliminated by the energy focussing provided by the migration.

The wavelet phase polarity can be also used to determine the presence of water. The phase of the wavelet is defined in this paper as the sequence of phase polarities as seen along a given trace. Figure 5 shows the end portion of the trace obtained at 35 m along the section shown in Figure 4. The trace was AGC gained and appears clipped at an arbitrary maximum. The AGC attempts to equalize the signals applying a gain which is inversely proportional to signal strength. Therefore it does not preserve relative amplitude information. The first of a series of phase polarity inversions occurs at 178 ns as seen in Figure 5. This gives the top of the water-filled fractured rock at about 7 m, about 1 m deeper than it appears to be in Figure 4. This discrepancy may be due to the uncertainty in recognizing the phase polarity sequence properly. This condition occurs when the leading edge of the wavelet cannot be ascertained due to closed spaced reflections. This may be the case on the top of the fractured rock.

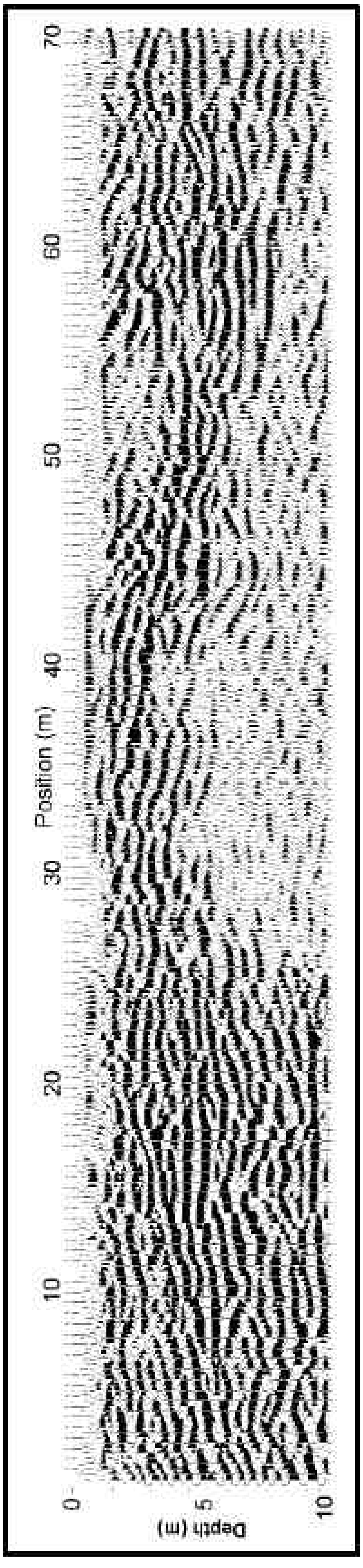

Figure 4. Migrated GPR section on crystalline rock. An uniform velocity of v_r=0.08 m/ns is assumed throughout.

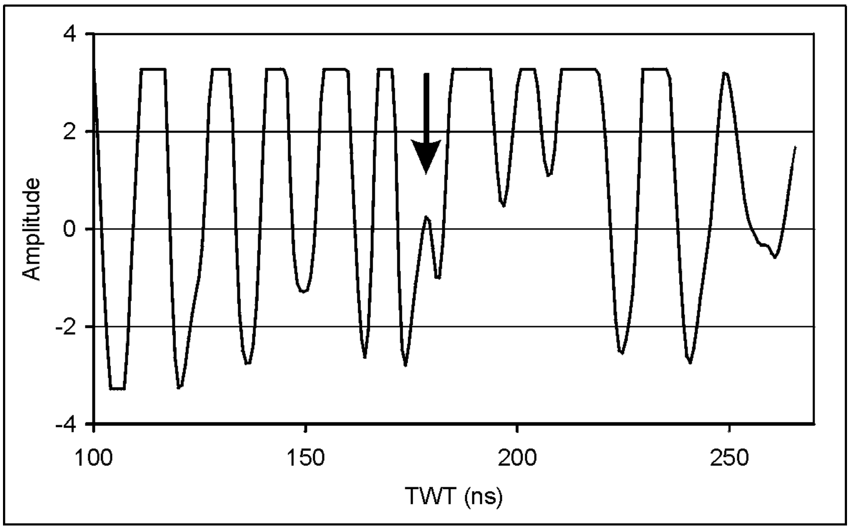

Figure 5. End section of trace at 35 m. The arrow shows the first of a series of phase inversions, occurring at the top section of the water-filled fractured rock. Amplitudes are clipped at a maximum of 3.2. The vertical scale is arbitrary.

INTERPRETATION

A great deal of effort in interpreting radar profiles goes into not only in understanding reflections and diffractions but also into deciphering of interference patterns. The focusing of energy provided by migration lighten that effort. The expected product is to recognize changes in reflector characteristics such as configuration, continuity, frequency and amplitude so to characterize radar facies. Radar facies are 3D regions representing particular combinations of physical properties like lithology, stratification, fracturing and fluid contents. Recovering the full geometry of such regions is not an issue here as we are dealing with a 2D profile, but with the data we can an idea of the layering of the gneiss and recover the contact between less and more fractured rock.

The section in Figure 4 gives a good image of the subsurface, revealing features such as the top portion of the water-filled fractured rock and the structure of the gneiss. The interpreted section is shown in Figure 6. The most prominent feature is the top of the fractured rock delimiting an extensive saturated zone (35 m wide), which is responsible for the high drainage rate of the spring.

In radar section of Figure 4 is possible to identify a series of semi-parallel folded reflectors all long the profile and small structures such as a lens shape between 0-30 m in the profile that is very similar to boudin structure (*B* in Fig. 6). The overall pattern of the reflectors along the profile resembles a migmatitic texture, with alternated veined/folded mafic (biotite/hornblende) and felsic layers (quartz). Another important feature identified are the sub-vertical fractures (*F* in Fig. 6) that occurs all long the section, these fractures are the main conduits to water ascension in the area.

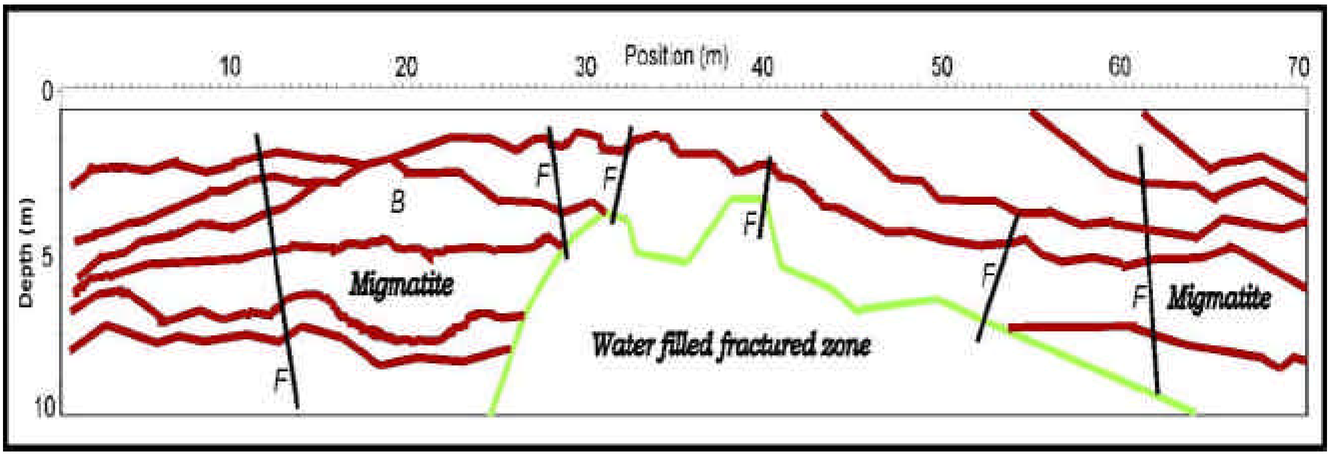

Figure 6. Interpretation of the radar section shown in Figure 4. *F* are interpreted fractures and *B* is interpreted as a boudin structure.

Independent geophysical data is in accordance with the GPR data. An 1-D interpretation of one VES positioned 42 m along the profile indicates a 4-layer earth (S. Berrino, personal communication, 1997). The 1-D model starts from top to bottom with a 2 m layer of 1500 ohm.m, followed by a 5 m layer of 3000 ohm.m and then to a saturated zone of 300 ohm.m that may extend down to 50 m, well beyond the penetration depth of the GPR data. The resistivity of saturated zone is basically the same of the water (2.9×10^2 ohm.m), indicating a high degree of fracturing and connectivity. A half-space of highly resistive fresh rock terminates the model. The first layer is constituted of saprolite and its thickness agrees with the estimated thickness of the superficial layer that contributes to the transfer of the direct wave energy (1.6 m for 100 MHz and a distance transmitter-receiver of 10 m) and what is seen in road cuts. The second layer is probably constituted fractured rock on the top of the saturated fractured zone.

CONCLUSIONS

This work presents the results from a GPR survey done for water exploration on crystalline terrain (migmatized gneiss). Reflection data was collected with the fixed offset configuration along a profile 70 m long. The velocity was estimated doing velocity analysis on CMP data. The estimated velocity value was 0.08m/ns. This value is 38% less than the tabulated velocity for granite-gneiss and is attributed to high water content in rock.

In the radar profile the water filled fractured zone is clearly outlined by a wide (35 m) region of lower amplitude values. The depth to the top of this saturated zone is variable along the profile (3 to 10 m). The presence of water in the fractured zone can also be mapped from inversion on the polarity of the wavelet phase at the radar traces. Independent geophysical data from a VES sounding are in accordance with the results obtained in this work. The GPR data provided a detailed characterization of shape and extension of the saturated zone. The GPR method demonstrated to be a powerful tool for underground water exploration in crystalline terrain.

REFERENCES

Beres, M., Haeni, F.P., 1991. Application of ground-penetrating-radar methods in hydrogeologic studies. *Ground Water* **29**, 375-386.

Cardimona, S., Clement, W.P., Kadinsky-Cade, K., 1998. Seismic reflection and ground-penetrating radar imaging of a shallow aquifer. *Geophysics,* **63**. 1310-1317.

Davies, J.L., Annan, A.P., 1989. Ground-penetrating radar for high-resolution mapping of soil and rock stratigraphy. Geopys. Prosp. 37, 531-551.

DNPM, 1997. Principais depósitos minerais do Brasil. v4 - Rochas e minerais industriais. Schobbenhaus, C, Queiróz, E.T., Coelho, C.E.S. (Coordenadores). Coordenador. Departamento Nacional de Produção Mineral (DNPM). Brasília. 9 - 38.

DNPM, 1998. Mapa geológico do Estado do Rio de Janeiro, escala 1:400000. Fonseca, M.J.G. Coordenador. Departamento Nacional de Produção Mineral. 141p.

Drews, M.G.P. 1998. Eletrorresistividade aplicada à prospecção hidrogeológica de terrenos cristalinos na região amazônica. In: SBG, Congresso Bras. Geologia, 40, Belo Horizonte, Anais, 1: 345.

La Terra, E.F., Menezes, P.T.L., Fontes, S.L., Germano, C.R. 1998. Aplicações de métodos eletromagnéticos para estudos de água subterrânea em prospectos não condutivos: estudo de caso em diques de diabásio. In: SBG, Congresso Bras. Geologia, 40, Belo Horizonte, Anais, 1: 381.

Martins, A . M.; Maurício, R.C.; Pereira Filho, J.C.; Caetano, L.C., 1997. Águas minerais do Estado do Rio de Janeiro. Departamento de Recursos Minerais (DRM), Niterói. 90p.

Mello, L.C, Mothé Filho, H. 1993. Geoeletricidade da baixada Santa Cruz/Itaguaí, campus da UFRJ: Potencial hídrico subterrâneo e de areias. In: SBGf, CISBGf, 3, Rio de Janeiro, Anais, 2: 405-409.

Metello C.M.S., La Terra, E.F., Fontes, S.L., Lages, F., Feijão, E., Borghi, L 1998. Aspectos geofísicos do Grupo Serra Grande (Bacia do Parnaíba) na região de São Raimundo Nonato (Estado do Piauí) - método magnetotelúrico. In: SBG, Congresso Bras. Geologia, 40, Belo Horizonte, Anais, 1: 381.

Oliveira, R.B..B. 1993. O uso da sondagem elétrica Schlumberger na prospecção de água subterrânea no cristalino do sudoeste da Bacia. In: SBGf, CISBGf, 3, Rio de Janeiro, Anais, 2: 421-423.

Rigoti, A., Corrêa, F.S., Katbeh, A. 1998. Prospecção Geofísica de aquíferos fraturados na Fm. Furnas. In: SBG, Congresso Bras. Geologia, 40, Belo Horizonte, Anais, 1: 35.

Van Overmeeren, R.A., 1994. Georadar for hydrogeology. *First Break*, **12**, 8, 401-408.

Yilmaz, O., 1987. Seismic data processing, SEG series: Investigations in Geophysics, vol. 2., S.M. Doherty, ed., SEG, 526p.